Numerical and experimental development of the DIKWE wave energy converter

Marc Le Boulluec, Michel Répécaud, Martin Trasch, Vincent Perier, Gaspard Fourestier, Philippe Magaldi, Margot Bremaud, Timothée Santagostini, Quentin Henry

2nd Maritime Engineering Meeting
Caen, 18 to 20 June 2024

Marc Le Boulluec Marc.Le.Boulluec@ifremer.fr

NUMERICAL AND EXPERIMENTAL DEVELOPMENT OF THE DIKWE WAVE ENERGY CONVERTER

Authors: Le Boulluec Marc[1], Repecaud Michel[1], Trasch Martin[1], Perier Vincent[1], Fourestier Gaspard[2], Magaldi Philippe[2], Remaud Margot[2], Santagostini Timothée[2], Henry Quentin[3]

[1]Ifremer, Centre de Bretagne, 1625 Route de Sainte-Anne, 29280 Plouzané, France
[2]GEPS TECHNO, 1 Rte de la Croix Moriau, 44350 Guérande, France
[3]Groupe Legendre, 5 Rue Louis Jacques Daguerre, 35136 Saint-Jacques-de-la-Lande, France

RESUME *:*

Le concept DIKWE vise la protection des côtes et des installations portuaires et la génération d'énergie par conversion de l'énergie des vagues.

Le système est composé d'un volet semi-immergé exposé face aux vagues qui oscille autour d'un axe horizontal situé en partie haute. Une chambre située en aval présente une surface libre dont les dimensions sont choisies en fonction des états de mer les plus probables sur le site considéré.

Les vagues incidentes interagissent avec le volet et induisent un mouvement d'oscillation du corps solide couplé avec l'écoulement dans la chambre. Un capteur d'énergie (Power Take Off) est connecté à l'axe de rotation du volet.

Le développement et la validation du concept DIKWE comporte trois phases :

Phase 1 : essais préliminaires dans le bassin de l'Ifremer Centre de Bretagne à une échelle 1/15. Le niveau de maturité technologique TRL 3 a été atteint [Le Boulluec et al. 2022].

Phase 2 : essais à une échelle intermédiaire d'une cellule isolée sur le site de Sainte Anne du Portzic opéré par l'Ifremer. Le TRL 6-7 est ainsi atteint. L'article détaille cette phase 2.

Phase 3 : essais d'un pilote à pleine échelle sur une digue de protection. Le TRL objectif sera 8-9.

Des résultats numériques et expérimentaux sont comparés. Ceux-ci comprennent l'énergie captée au regard des vagues observées sur site, du niveau de marée et des paramètres du PTO. Les puissances mécanique et électrique sont établies. Les perspectives du développement à pleine échelle sont décrites.

MOTS CLEFS : Hydrodynamique, Vagues, Energie, Conversion, Côtier.

ABSTRACT:

The DIKWE concept aims at protecting coastal and harbours installations and generating energy from Wave Energy Conversion.

The device consists of a semi-immersed flap facing the waves and oscillating around a horizontal axis located at its top. A chamber with a free surface which dimensions are tuned according to the most probable sea states characteristics on the considered site is located behind the flap.

The incoming waves interact with the flap and induce an oscillating motion of this rigid body coupled with the water flow in the chamber. A Power Take Off is connected with the flap rotating axis.

The development and step by step validation of the DIKWE concept includes three phases:

Phase 1: preliminary calculations and tests at Ifremer ocean engineering basin at model scale 1/15. The Technology Readiness Level reached is 3[Le Boulluec et al. 2022].

Phase 2: tests of an intermediate scale single cell device in Sainte Anne du Portzic sea test site operated by Ifremer. The TRL is 6-7. The article reports on the phase 2 of the project development.

Phase 3: full scale pilot included in a protecting dyke. The target TRL will be 8-9.

Numerical and experimental results are compared. The results are energy captures according to the recorded waves on the test site, the tide level and the parameters of the PTO. Both mechanical power on flap axis and electrical power are assessed. The perspective at full scale development is described.

KEYWORDS: Hydrodynamics, Waves, Energy, Conversion, Coastal.

1. INTRODUCTION

The DIKWE concept aims at protecting coastal and harbours installations and generating energy from Wave Energy Conversion [Le Boulluec et al. 2022].

The device consists of a semi-immersed flap facing the waves and oscillating around a horizontal axis located at its top. A chamber with a free surface which dimensions are tuned according to the most probable sea states characteristics on the considered site is located behind the flap.

The incoming waves interact with the flap and induce an oscillating motion of this rigid body coupled with the water flow in the chamber. A Power Take Off (PTO) is connected with the flap rotating axis.

The main geometrical parameters of the DIKWE concept are the height and width of the flap, the horizontal length and width of the chamber, and the vertical level of the system which may vary according to the possible tidal effects.

This coupled system (flap, chamber, PTO) can be installed on dykes or can be parts, when included in a concrete caisson, of a new dyke. The PTO can be located in the building enclosing the device.

The development and step by step validation of the DIKWE concept includes three phases:

- Phase 1: preliminary calculation and tests at Ifremer ocean engineering basin at model scale 1/15. The Technology Readiness Level reached is 3 [Le Boulluec et al. 2022].
  During this phase the PTO was made with an aeraulic compression system connected to flap axis and a nonlinear damping was applied. The conclusion of the tests was satisfying enough to step to phase 2.
- Phase 2: tests of an intermediate scale single cell device in Sainte Anne du Portzic sea test site operated by Ifremer. The device is isolated and located upstream the local dyke and operated for water level above the mid tide level. The target TRL is 6-7. The PTO is made of a hydraulic device which is technically close to a full-scale device technology.
- Phase 3: full scale pilot included in a protecting dyke. The targeted TRL will be 8-9.

The present article focuses on some of the results of the 2nd phase of the project.

2. EXPERIMENTAL INFRASTRUCTURE

The Sainte Anne du Portzic test site is located near the Strait of the Bay of Brest and is protected from the offshore waves (Figure 1). The waves heights are reduced by a scale around 10, but the waves periods and the wind speed remain similar to the open sea configuration [Träsch et al. 2023]. Local current may reach 2 knots at the periphery of the site and less than 1 knot at prototype location.

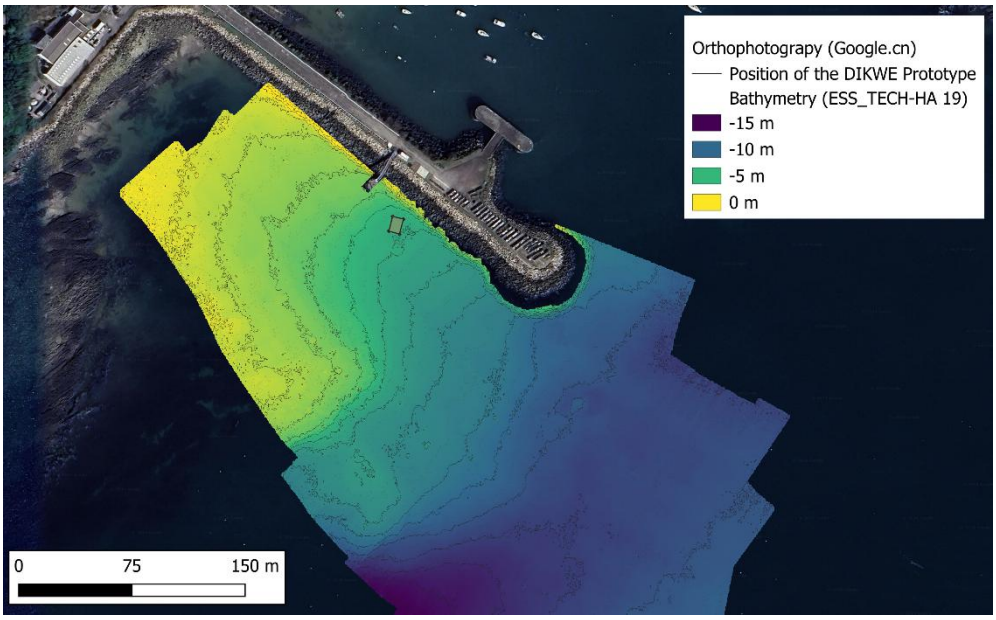

Figure 1: Bathymetry map at Sainte Anne du Portzic test site

Incoming waves are measured by wave sensors, most of the time SPOTTER SOFAR Technology (Figure 2). The main direction of waves during energetic events is S-SW. Quiet and stronger events alternate and the influence of the tide level can be observed with oscillating significant wave heights.

Pressure sensors are used to evaluate mean values of the water level which varies with the tide dynamics. The maximum tide margin on the site exceeds 6 m. It should be noted that Brest is the reference harbour for the tide level and chronology in France.

Anemometers located on the dyke protecting the leisure harbour located north of the test site record the wind velocity and direction. ADCP have been used to evaluate the current dynamics at several points on the site. In the case of these DIKWE tests, the wind and current velocities are not considered as key parameters for the dynamics and efficiency of the system.

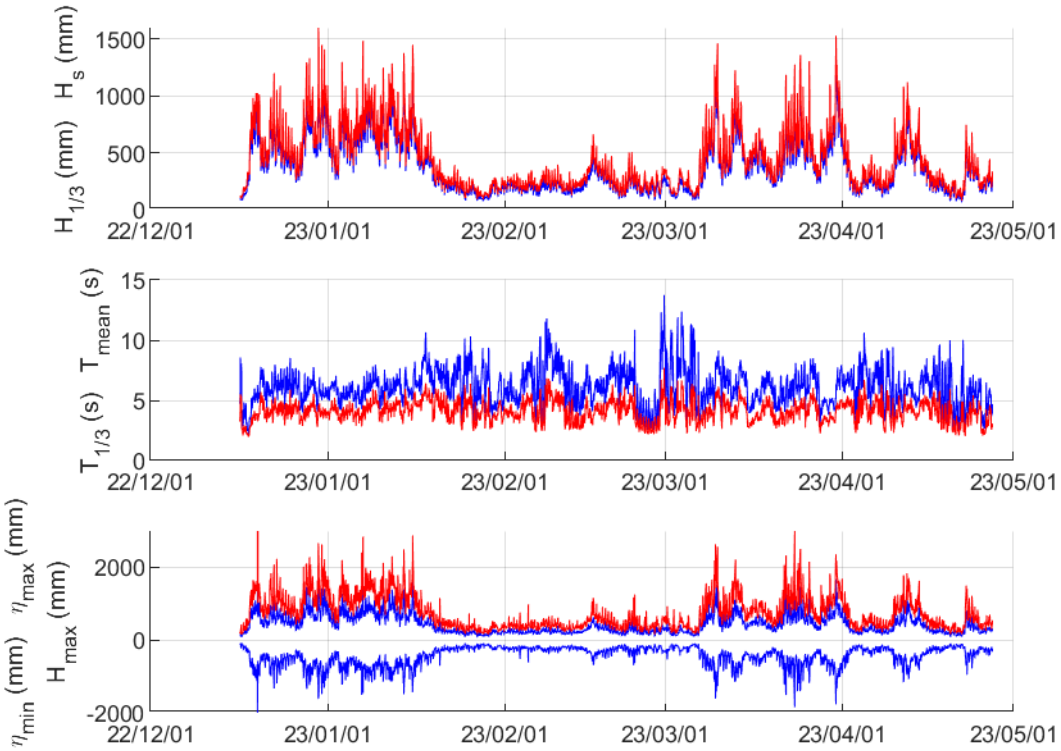

Figure 2: Wave elevation in Sainte Anne du Portzic test site during a period of time included in the DIKWE tests. Data delivered by SPOTTER/SOFAR wave sensor.
All parameters from wave by wave analysis except H_s from spectral analysis.
$H_{1/3}$, $T_{1/3}$, η_{min}, η_{max} (blue lines)
H_s, T_{mean}, H_{max} (red lines).

2. DIKWE DEVICE

The system installed at sea during the phase 2 project is an isolated one. A jacket is first installed in a water depth around 5.5 m at low tide. At mid tide, the top of the jacket is just immersed (Figure 3). The DIKWE module itself is then connected at the top of the jacket and is able to work for the upper tide levels and at low tide levels the device can be accessed for maintenance and inspection (Figure 3). The stability of the whole system is obtained by gravity loads (160 additional tons of steel are located at the bottom of the jacket). The DIKWE prototype is oriented at a constant heading (around 202° from true north) to capture the highest waves on site by their interaction with the flap, only moving part of DIKWE system. Its location is approximately: -4.5520° East, 48.359° North.

Figure 3: Jacket and DIKWE

On board instrumentation

Dikwe prototype is instrumented to understand the power production at different stage form the incident waves power to the energy on the generator shaft. The following measure are performed:

- Two pressure sensors are placed respectively inside the chamber and just in front of the flap at the middle of the prototype. These two sensors allow the measurement of the waves and sea water level on the system.
- The flap inclination angle is measured by two sensors one on each side of the flap.
- The pressure in the hydraulic circuit is measured with one sensor just before the hydraulic motor.
- Tension and electrical current are measured on the electrical generator. The rotational velocity and the mechanical torque on the generator shaft are derived from these measurements. The mechanical power on generator shaft is deduced from the rotational velocity and the torque.

The mechanical torque on the flap can be assessed from the pressure in the hydraulic circuits and the geometrical characteristics of the hydraulic cylinder (surfaces of the pistons, geometrical positions of the connections). The mechanical power on the flap axis is assessed from the mechanical torque calculated above and flap's rotational velocity (evaluated from flap position after an appropriate filtering).

The torque applied by the generator on the system is kept proportional to the generator rotational velocity. The proportionality factor is modified as follows:

- In the first part of the tests, the proportionality factor is kept constant all over the period. During this part, a constant value close to the best proportionality factor numerically tested is used.
- In the second part of the tests, the proportionality factor is modified every 5 min or 10 min to sweep various values against different environmental conditions.

This paper concentrates on the first part of the tests.

Measure examples

For example, the water level measured with the pressure sensor at the bottom front of the system on September 7th 2022 is shown on figure 4. The tide signal is clearly seen and corresponds to the high tide time and low tide time at Brest shown in table 1. Below a water depth of 9.40 m, the system is off and out of the water (period between 4 am and 10 am and between 5 pm and10pm). The acquisition system has been restarted this day which is traduced in a short stop in the measurement between 1pm and 2pm.

Table 1. Timetable of tides at Brest on September the 7th 2022. Time data are in UTC time zone. Data extracted from the SHOM website maree.shom.fr

	Time	Heigh (m)
Hight tide	1:02	5.69
Low tide	7:19	2.41
Hight tide	13:31	6.16
Low tide	19:54	1.96

On top of the tide signal there is a high frequency oscillation that can't be clearly seen on one day plot which correspond to the waves perturbed by the system. As it can be seen on figure 5 that day waves do not change much with a significant height around 0.4 m. This prototype has been designed to work with significant heights between 0.2 m and 1 m. Hence this day correspond to usual working waves.

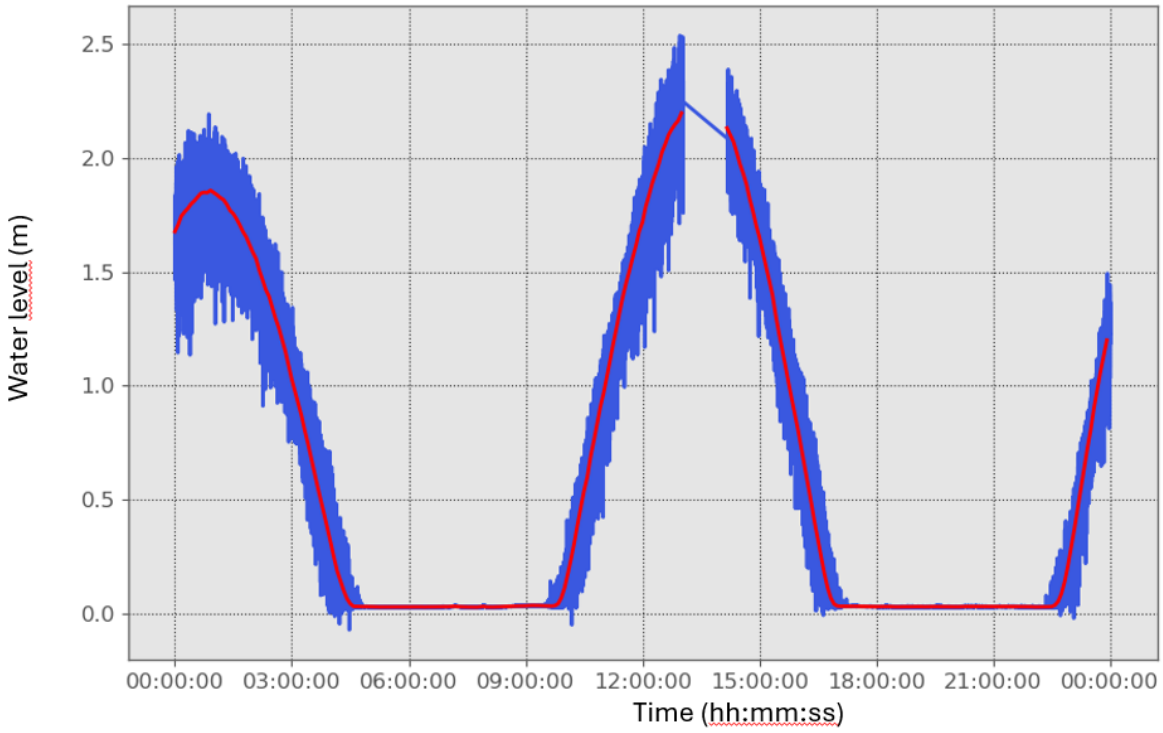

Figure 4: Typical measurement of the sea water level measured on the 07/09/2022 with the pressure sensor at the front of the system. The blue line is the raw data, the red line is the sliding mean over 5 minutes.

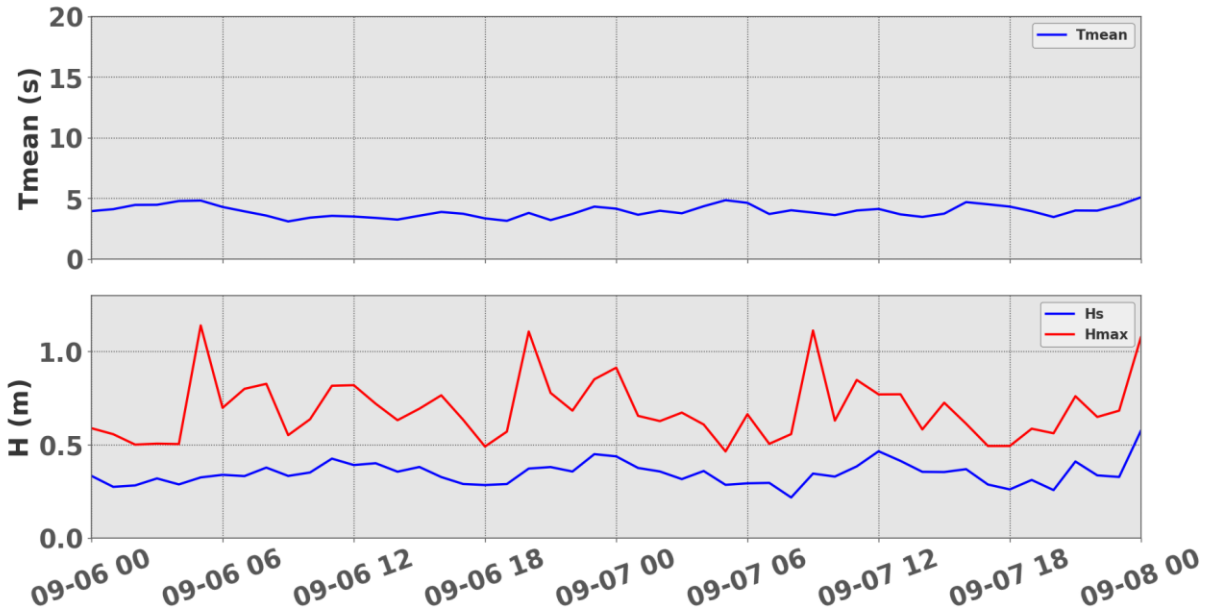

Figure 5: Waves measured next to the prototype measured on the 06/09/2022 and 07/09/2022.

The angle taken by the flap under these waves is presented on figure 6.This day, angles as high as 30° are taken and the ten minutes mean mechanical power extracted on the flap axis is up to 1.4 kW (figure 7).

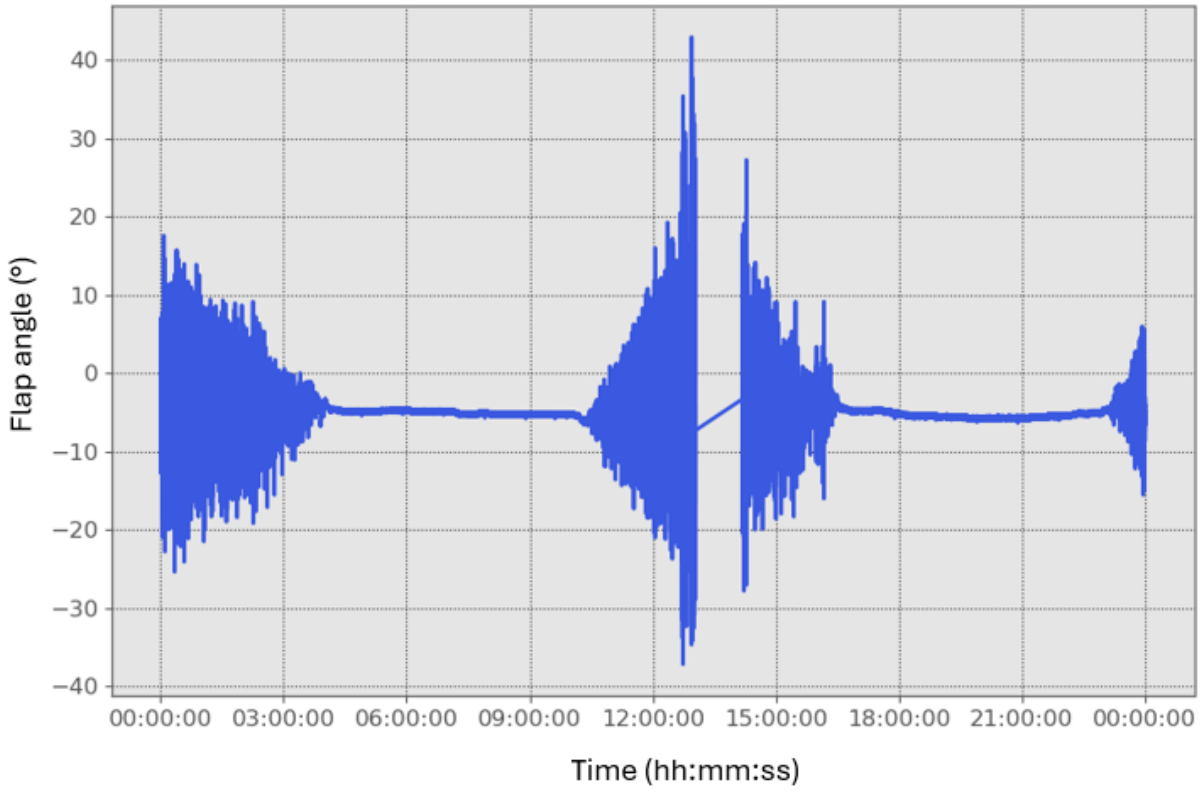

Figure 6: Measurement of the flap angle around its axis on the 07/09/2022

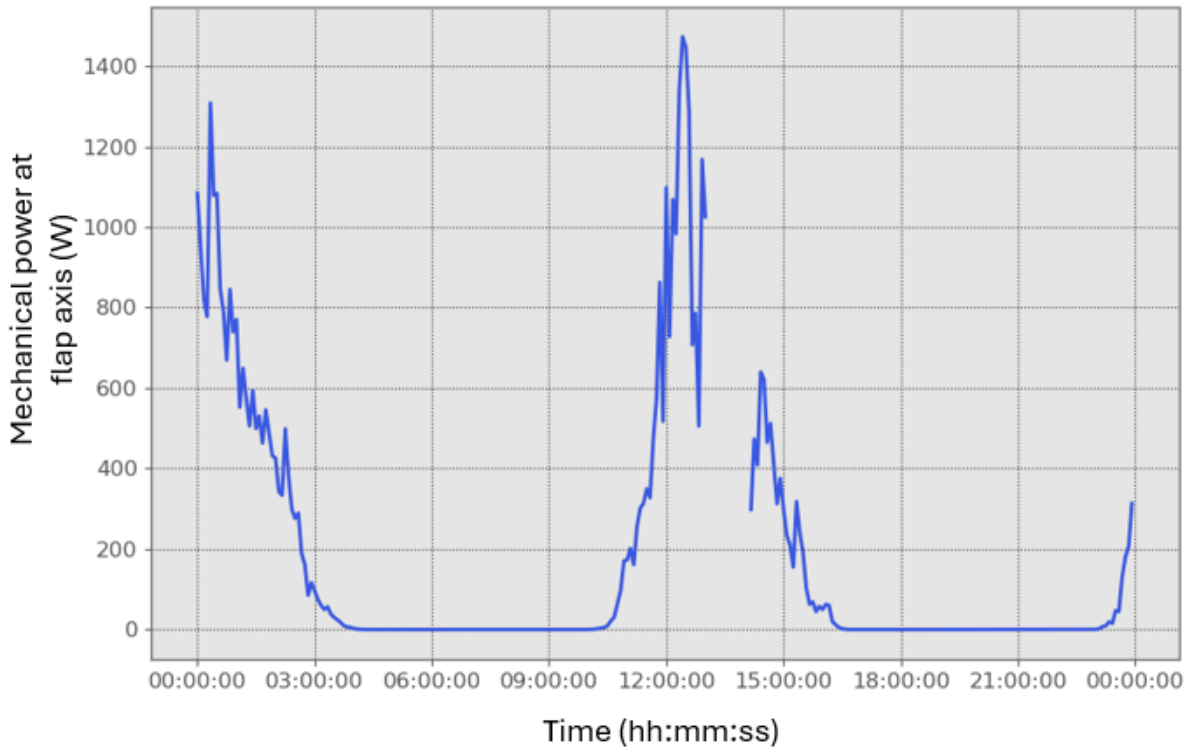

Figure 7: Measurement of 10 min mean mechanical power on the flap shaft in Watt on the 07/09/2022.

The hydrodynamic efficiency η (in %) is defined as:

$$\eta = \frac{P_G}{P_h B}$$

Where P_G is the mechanical power (in W) at the flap shaft and P_h is the wave power by crest length (in W/m) and B is the width of the system. The influence of the water level on this efficiency is clearly seen on figure 8. On this figure, each point shows the hydrodynamic efficiency calculated over a 10 minutes sea state as a function of the 10 minutes averaged water level. For water level below 0.5 m the flap is not in the water and no power is produced. For water levels between 0.5m and 2m, the efficiency increases linearly with the water level. For water level above 2.5m the efficiency still increases but with a wider distribution and another proportionality factor.

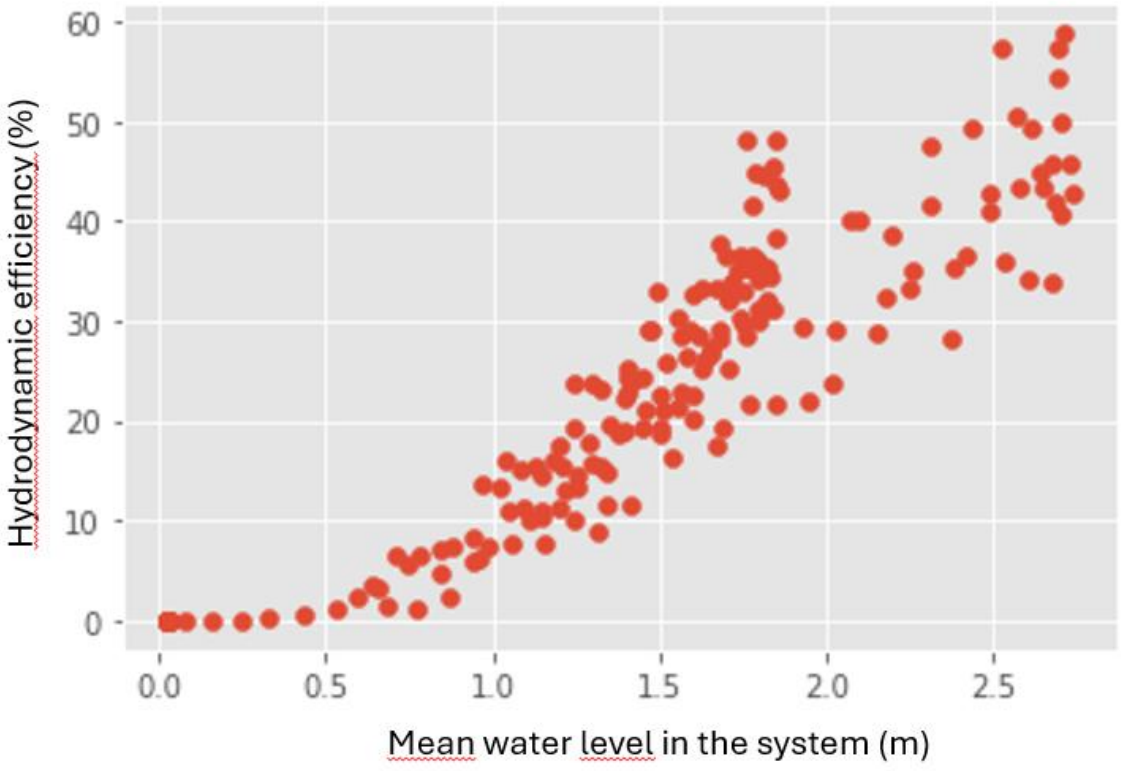

Figure 8: Hydrodynamic efficiency of the system as a function of the mean water level

4. Numerical modelling

Linear Method

The basic modelling is based on the Boundary Element Method under the assumption of a perfect fluid, a small free surface elevation and a small flap angular motion. The boundary conditions at first order of development are linear. Body number 1 is the fixed main structure and body number 2 is the moving flap which reference point is located on the middle of the axis of rotation. A mesh made with quadrilateral facets supporting constant singularities is generated (figure 9). The results of the so-called Diffraction and Radiation method are F_w (diffraction of the incoming waves by the fixed bodies), M_a and B (radiation by the moving bodies in calm water).

F_w: wave forces (12x1 vector)
M_a: added masses (12x12 matrix)
B: linear wave damping (12x12 matrix)

Additional results consist in the free surface elevation. This gives particular information on the free surface effects inside the chamber.

The wave forces and moments are used for assessing the stability of the structure under the waves loads. The simple dynamics equation for the angular pitch motion of the flap (degree of freedom number 11) around its axis is:

$$\left(M_{11,11} + M_{a11,11}\right)\ddot{X}_{11} + \left(B_{11,11} + B_{l11,11}\right)\dot{X}_{11} + K_{11,11}X_{11} = F_{w11} + F_{R11}$$

$$F_{R11} = -B_{PTO}\dot{X}_{11}$$

where $M_{11,11}$ is the mass inertia of the flap, $B_{11,11}$ is an additional linear damping related to hydrodynamics and mechanical friction, $K_{11,11}$ is the stiffness of the flap under the action of its weight and buoyancy, F_{R11} is the action of the linear PTO on the flap axis and X_{11} is the pitch angle.

Moreover, additional dissipation is inserted in the model to prevent violent resonant motion and simulate viscous damping. However, as stated in Hydrostar's manual [Bureau Veritas, 2021], the dissipation parameters are artificial and should be calibrated.

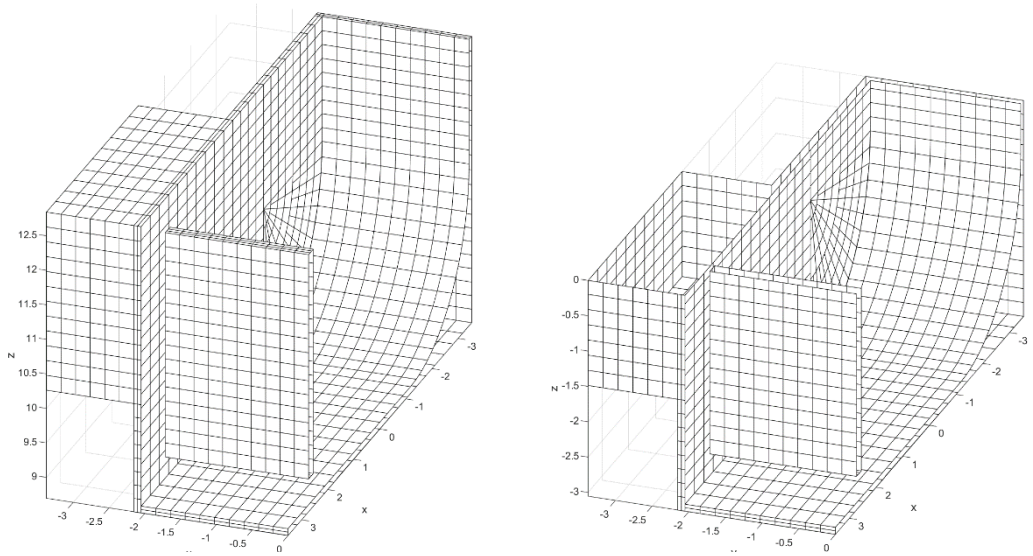

Figure 9: mesh with facets of the flap and the main body for linear boundary element method.
Left: full bodies with elevation from the sea bottom.
Right: bodies limited to the free surface with calm water level at 11.75 m

Nonlinear Method

The WEC is modelled in the computational fluid dynamics (CFD) software OpenFOAM with the add-on NavalHydroPack developed by H. Jasak and his team [Wikki, 2021]. The following hypothesis are made in the model setup:

- The sea water motion is assessed solving numerically the Navier Stokes equations. The sea water is supposed to be incompressible.
- The flow is considered laminar. Hence no turbulence model is used.
- . The free surface is modelled using the Gost fluid method [Vukcevic et. al., 2017]
- The flap is modelled using the overset technique [Benek et. al., 1983]
- The boundary conditions on the flap and on the fixed part of the system is a no slip condition.
- The seabed is considered horizontal with the depth equal to the depth at the prototype measured by the pressure sensor in front of the flap.
- The dyke behind the prototype is not modelled.
- The calculation is performed in two dimensions. Any tridimensional effect is ignored. Especially, the waves spreading is ignored and any angle between the wave propagation axis and prototype's axe is ignored.
- The waves spectrum measured next to the system is used as boundary conditions for the input. In this process, the exact wave order is not preserved.
- The water level fixed in the numerical model is equal to the mean water level measured.

- The jacket holding the prototype is not depicted.
- The detailed shape of the flap is not represented in the model. It is represented with a simple rectangular shape. Hence the immersed volume is higher than the real one. The mass of the flap is set up to represent well the flap's density.
- The power takeoff impact on the flap is modelled as a simple damping coefficient on the flap.

Figures 10 and 11 show respectively a schematic view of the calculation domain and the mesh grid next to the prototype.

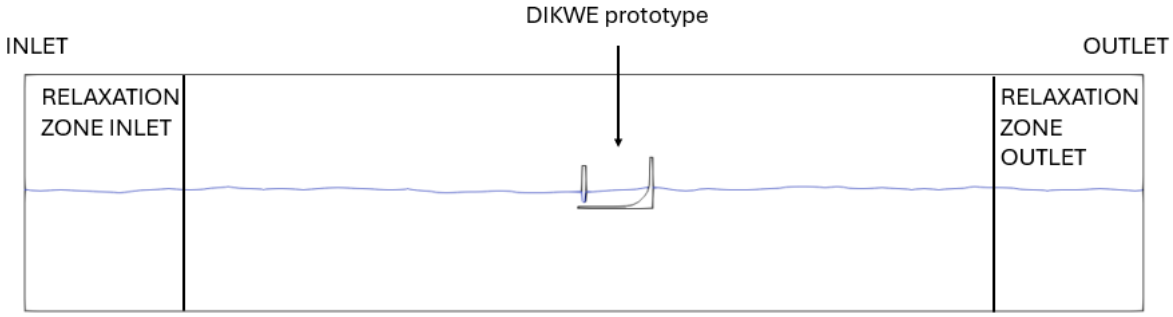

Figure 10: Schematic view of the calculation domain.

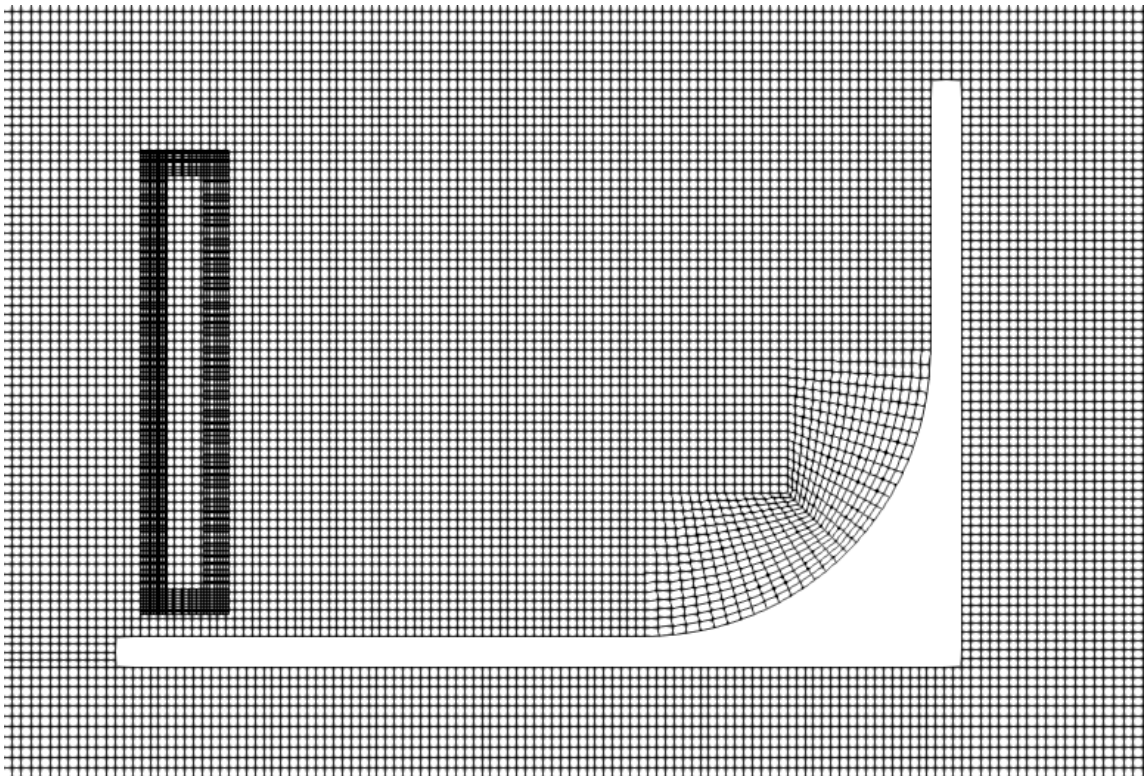

Figure 11: Mesh grid next to the prototype.

5. Comparison between numerical and experimental results

A set of periods of time have been identified as interesting data (table 2). Measurement from these instants have been extracted and set up as input data for numerical models. Then a comparison between the measured data and the numerical results is

performed.

Table 2. set of periods of time selected

Name	Date	Hs (m)	Te (s)	Water level in the device (m)	Wave heading (°)
1	06/09/22 23:30	0.51	6.4	1.48	192.9
2	06/09/22 23:40	0.62	6.9	1.55	189.6
3	07/09/22 00:00	0.59	6.4	1.69	187.3
4	07/09/22 01:00	0.44	4.8	1.84	198.9
5	07/09/22 01:30	0.40	5.1	1.74	203.8
6	07/09/22 02:10	0.42	5.5	1.49	204.7

At all these instants, the RAO (Response Amplitude Operator) of the flap is calculated from the measurements. Numerical models are performed using the water level, waves significative heights and periods given in table 2 as input. The flaps RAO are calculated with these models and compared to measurements data in figure 12 and 13.

Figure 12 shows the comparison between measurements and the two numerical models for event number 4 in table 2. The CFD model shows a very good agreement with the measurements for short periods. Up to 7.5s, the CFD model follows the variations in the measured RAO. However, around 10s, next to RAO's maxima, the CFD model present discrepancies with the measurements up to 40%. The reasons of this discrepancies are discussed below. The linear model has been calibrated with the measurements. The calculation is performed with various values of the dissipation parameter and the best approximation is retained. For period under 9 s, the linear model shows higher discrepancies with the measurements than the CFD model (difference around 40% for the linear model and around 10% for non-linear one at 6 s). The RAO maximum around 10s, is better described by the linear model, with differences around 3% at 10 s. However, the linear numerical RAO is much sharper than the measured one.

In figure 13, the comparison between measured RAOs and calculated ones with the non-linear model are presented for various sea states. As in figure 12, the order of magnitude of the measured RAO is found numerically. And the agreement for periods below 8s is very good (discrepancies around 10% or less at 6s for any sea state). As in Figure 12, there is higher discrepancies in describing the maximum value of the RAO. Moreover, a much larger variability is observed in the on-site data than in the numerical data. The flap RAO is under-estimated for the two highest water level studied and over-estimated for the others. The two highest water levels are also the two shortest wave periods. Many reasons shall explain discrepancies of the numerical model. First the wave direction and wave spreading are not taken into account in the numerical model. These 3D effects could explain the greater variability of the on-site data. For example, a sea state with a mean direction correctly oriented but with a wide spreading should result in smaller flap's motion and smaller power production level than the same sea state without spreading.

Another explanation is the natural variability of the waves that is not fully assess in the numerical models. The wave sequence in input of the numerical model is arbitrarily chosen. Moreover, the sea state length is quite short (10min), and the wave spectrum is not fully represented in this duration. Such a short length has been chosen as a balance between two constraints:

- On one side, the longer is the sea state the better it is represented.

- On the other side, the shorter is the sea state the more constant is the sea level resulting in a constant behaviour of the flap over this sea state.

Indeed, as seen in figure 8, the flap's behaviour is changing with the water level. During, spring tides the water level can rise at velocities higher than 1 m/h or 0.25 m by 15 minutes or 0.17 m by 10 min. The sea state is kept constant over all campaign and chosen to 10 min.

Another main discrepancy, between the numerical model and the real system is the Power Take Off behaviour. In the numerical model it is considered as a constant linear damping coefficient whereas in real system there is complex hydraulic system with non-linearities.

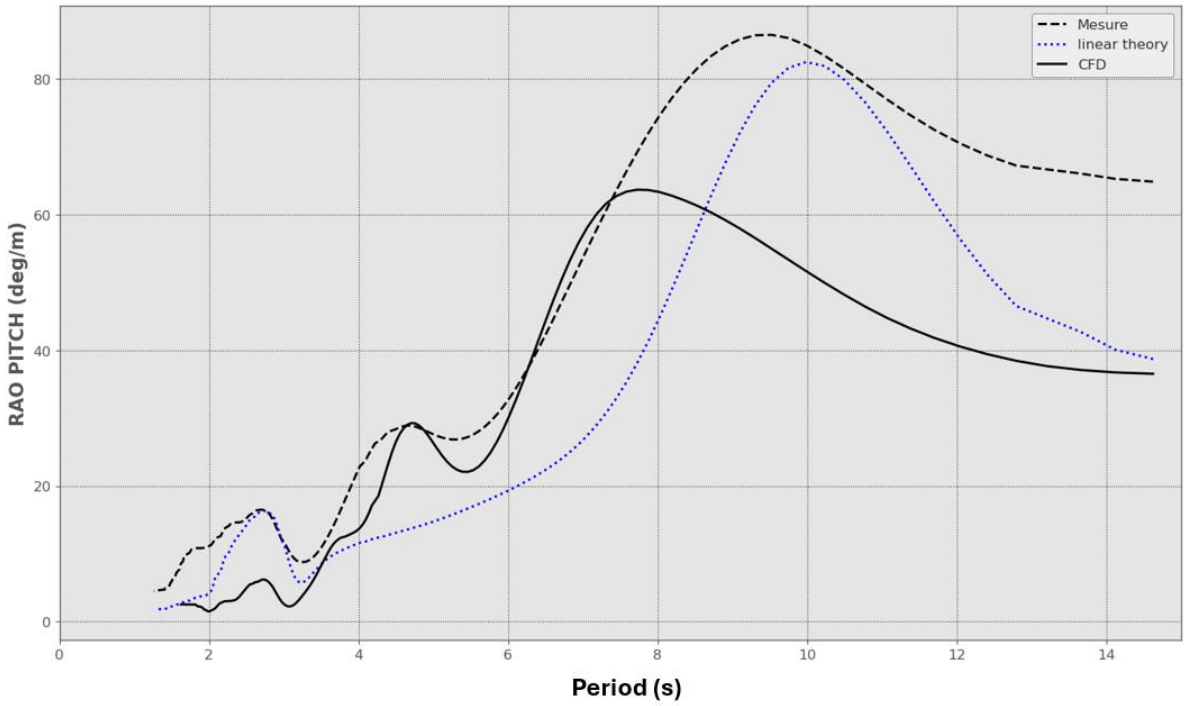

Figure 12: RAO of the pitch of the flap. Comparison between measurements (black dashed line) linear model (dotted blue line) and non-linear model (continuous black line) for selected event number 4

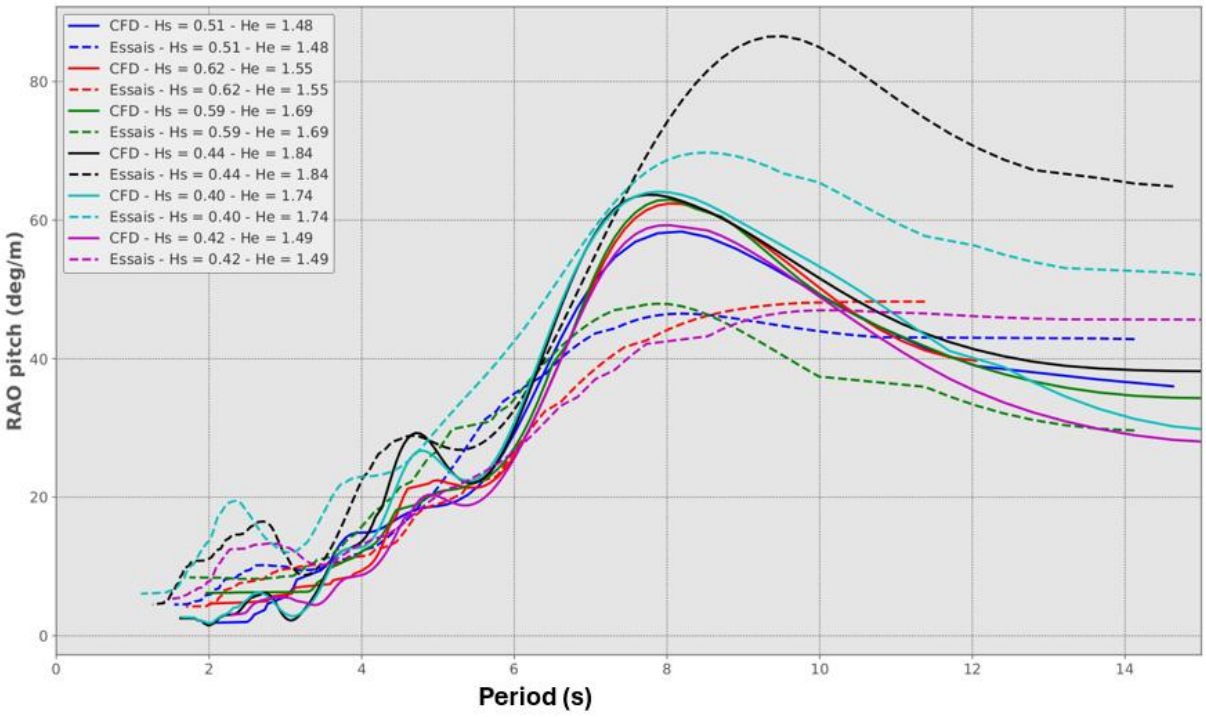

Figure 23: RAO of the pitch of the flap. Measurements are in dotted lines; numerical values are in continuous lines.

6. CONCLUSION

The tests run on the Sainte Anne du Portzic sea test site on an intermediate scale of the DIKWE concept leads to several conclusions:

- Thanks to environmental measurements and monitoring of the PTO, the results obtained during wave tank testing were confirmed. The power production was found to be close to the expected power extraction. The power production was encouraging with mean mechanical power of up to 4.5kW.
- The hydraulic PTO installed is similar to the one that could be installed on a commercial system.
- The tests at intermediate scale allowed to test, improve, and detect future improvements of the installation process, maintenance program and monitoring of the system (keeping in mind of the differences between the full-scale system and the prototype).
- Some observations could be made about the bio-fouling aspects.

The comparison between the numerical model and on site measured data shows that the order of magnitude of the flap's RAO is found numerically even though large discrepancies are observed at some instants. However, measured data are not as fully controlled as in wave flume tests and far more difficult to assess (see the results of the wave tests of phase 1 in [Le Boulluec et. al., 2022]). Some work is on going to improve this correlation. For example, follows a non-exhaustive list of the currently on going work : improve the modelling of the Power Take Off, other sensibility studies to better understand the prototype behavior, perform a similar analysis at other period of times to check if the conclusions are similar.

These results are promising. The next step (phase 3) of this project is to install a system composed by at least 3 units to reach TRL 8-9. This system is currently in a design phase. It is expected to be installed in the next years on the French coast.

7. ACKNOWLEDGEMENT

The DIKWE Phase 2 project received the support of the Brittany Region / Région Bretagne.

8. REFERENCES

Bureau Veritas, 2021, Hydrosar manual, version 8.3.beta

Le Boulluec M., Fourestier G., Repecaud M., Henry Q., Magaldi, Ph., 2022. *Projet DIKWE, la digue à énergie positive*. Conférence RIM 2022.

Trasch Martin, Raillard Nicolas, Perier Vincent, Le Boulluec Marc, Repecaud Michel, Matoug Camil (2023). *Metocean conditions at the Ifremer in situ test site in Brest*. 5th International Conference on Renewable Energies Offshore (RENEW 2022).

Vukcevic, V., Jasak, H., Gatin, I., 2017. *Implementation of the ghost fluid method for free surface flows in polyhedral finite volume framework.* Comput. Fluids 153, 1–19.

Wikki Ltd, 2021, http://wikki.co.uk/index.php/out-products/, consulted on 27/05/2024.

Benek, J., Steger, J., Dougherty, F.C., 1983. *A flexible grid embedding technique with application to the Euler equations.* In: 6th Computational Fluid Dynamics Conference Danvers. p. 1944.